

Characterisation of NdFeB magnet powder used for laser powder bed fusion

Yong Rong Chan^{1,2}, Sankaranarayanan Seetharaman², Jerry Ying Hsi Fuh¹ and Lee Heow Pueh¹

¹ College of Design and Engineering, National University of Singapore, 9 Engineering Drive Block EA #07-08, Singapore 117575
² Additive Manufacturing Group, Advanced Remanufacturing and Technology Centre, 3 Cleantech Loop, #01/01 CleanTech Two, Singapore 637143

KEYWORDS: Powder Characterisation, NdFeB, Laser Powder Bed Fusion, 3D Printing

Additive manufacturing of NdFeB magnet powder using the Laser Powder Bed Fusion process is an emerging area of interest with potential to improve electrical machines with design freedom. This technology is not only dependent on the use of optimised process parameters, but also on the characteristics of the powder being used and the powder's fitness for use over time or after recycling. However, current research about the characteristics of the NdFeB magnet powder used and the effect of powder reuse is still limited. The aim of the research was to characterize the NdFeB powder used in virgin condition and after one manufacturing cycle with a Concept Laser M2 Cusing machine. An in depth understanding of the powder characteristics will provide insight on powder behaviour and melt-pool during processing. To achieve the research's goal, the characteristics of the virgin and recycled NdFeB powder were investigated. It was found that there was an increase in particle size observed after just one time of recycling. Majority of virgin and recycled powders showed good sphericity, with some elongated particles and satellite particles found. Both conditions of powders tested also present a good flowability according to the Hausner ratio and angle of repose. The rheology and flowability of the powder were also tested using the FT4 rheometer and Revolution Powder Analyser to better understand powder behaviour during spreading in the Laser Powder Bed Fusion process.

1. Introduction

In the history of permanent magnets (PM), various types of PMs have been developed since 1930s, namely, the ferrite and Alnico PMs, followed by the Samarium Cobalt PMs and in the 1980s, the Neodymium (NdFeB) PMs which are the strongest among all the PMs. This gave rise to the wide use of NdFeB PMs as their strength enabled the miniaturization of various products used in modern applications.

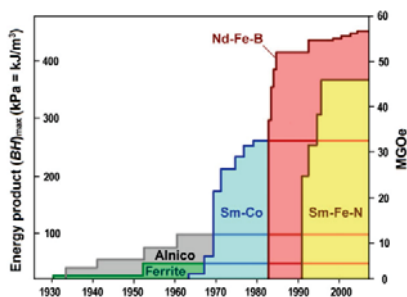


Fig. 1 Development of PMs over the years [1]

However, the manufacturing methods for NdFeB remain conventional in the form of spark plasma sintering (SPS) and injection molding (IM). Additive manufacturing (AM) of NdFeB is an emerging area with limited reported work exploring the design freedom and possibilities offered by AM. Design freedom offers the potential to overcome inherent limitations of the NdFeB which is its operating temperature as cooling channels can be printed with AM.

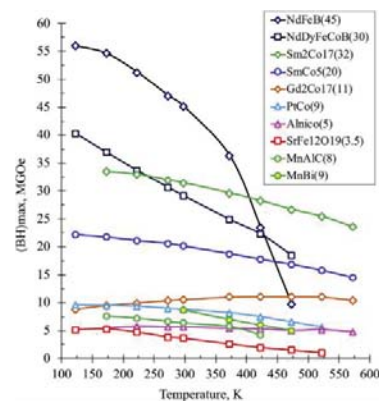


Fig. 2 Temperature dependence of (BH)max for PMs [2]



Figure 3. Cooling channel in NdFeB part fabricated using AM [3]

In addition to design freedom, AM also carries good potential to be a more sustainable alternative for RE PMs compared to conventional subtractive manufacturing technology. To enable this technology, it is important to optimise not only the process parameters but also understand better the material being used in this process.

2. Powder characterisation

2.1 Powder characteristics

The powder's rheology flow properties and packing density are important and key enabling characteristics required for the LPBF process. In LPBF, homogenous powder spreading is required to enable uniform energy absorption in the processing area [4]. This can only be achieved with good powder flowability when spread using apparatus such as a recoater.

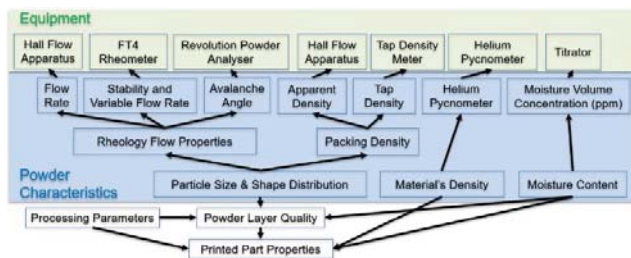


Fig. 3 Powder characterisation of materials in LPBF

Powder flowability can be attributed to numerous factors such as; particle size distribution (PSiD), particle morphology (shape distribution) and moisture content [5]. Therefore, it is important to assess contributing factors affecting the powder flowability.

The study of the effect of powder characteristics, especially with regards to particle size and shape distribution on final part properties is an ongoing complex area of research with compounding effects which affect powder fusion and melt pool efficiency as summarized in the figure below.

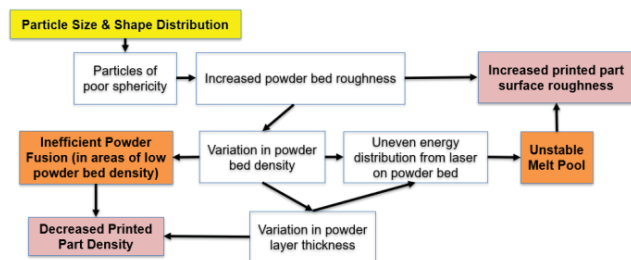


Fig. 4 Effect of poor particle sphericity on printed part quality

2.1.1 Powder of interest

The powder of interest in this paper is the MQP-S-11-9-20001 (MQP-S) powder manufactured by Neo Magnequench [6]. Determined by means of Energy Dispersive X-Ray Spectroscopy (EDX) and Scanning Electron Microscope (SEM), its composition is said to be Fe70.8–Nd18.2–Zr4.3–Co2.4–Ti2.2–Pr2.1 (composition in wt%) and the powder shape is spherical with minimal satellites [7,8,9]. The sphericity of the powder may be visualised in the figure below, extracted from a study by C. Huber et al. [10]

The powder being tested in this research is (i) the MQP-S powder in its virgin condition and (ii) the MQP-S powder after being used once where a part has been printed with it and subsequently collected to test with.

2.1.2 Trends on effect of powder characteristics

Balbaa et al. have found that fine particles of AISi10Mg ($D_{50} = 9\mu\text{m}$) produced parts with lower dimensional accuracy as compared to the coarser ones ($D_{50} = 40\mu\text{m}$). This phenomenon is said to be due to the higher inter-particle friction in the fine powder, causing poor powder flowability. Additionally, it was also mentioned that inhomogeneous spreading is a direct cause of poor powder flowability [11].

2.2 Methods

2.2.1 Method of collecting virgin powder

MQP-S powder was received in 2 bottles of 20 kg each where they were both sampled with a scoop in accordance with ASTM B215 - Standard Practices for Sampling Metal Powders.

2.2.2 Method of collecting powder to be reused

A print of 25 cubes was completed with parameters obtained from literature and the powder un-sintered in the build platform was collected after the print.

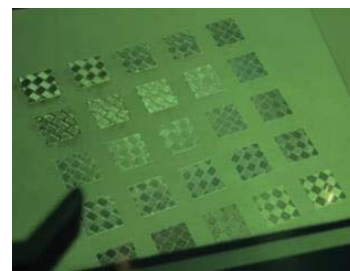


Fig. 5 Print of 25 cubes where powder to be reused was collected

2.2.3 Characterisation methods

The equipment used for powder characterisation is summarized in the figure and table below. Various equipment conventionally used for particle analysis have been used. Due to the limited availability of commercial powder characterisation equipment, these equipment sometimes used in the fast moving consumer goods and pharmaceutical industries have been used here today to give us an insight on the intrinsic and extrinsic characteristic characteristics of

the MQP-S powder, as well as its behaviour when subject to rheological forces using the Revolution Powder Analyzer equipment and FT4 Rheometer.



Fig. 6 Equipment used for powder characterisation

Table 1. Powder characterisation equipment and measured characteristics

Equipment	Characteristics
Malvern Morphologi G3	<ul style="list-style-type: none"> Particle Size Distribution Particle Shape Distribution
Horiba LA-960	<ul style="list-style-type: none"> Particle Size Distribution
FT4 Powder Rheometer	<ul style="list-style-type: none"> Stability and variable flow rate Shear Test Aeration Test
Hall/Carney Flow Meter	<ul style="list-style-type: none"> Flow rate Apparent Density Angle of Repose
Arnold Meter	<ul style="list-style-type: none"> Apparent Density
Revolution Powder Analyser	<ul style="list-style-type: none"> Avalanche Angle
Tapping Machine	<ul style="list-style-type: none"> Tapped Density
Helium Gas Pycnometer	<ul style="list-style-type: none"> True Density

2.3 Results

Results for the virgin powder show that there is minimal bottle-to-bottle variation with a thorough understanding of the powder characteristics achieved as shown in the figure below.

Among all the information gathered with the extensive testing completed, the key take away is that the Neodymium powder has a size range of 19 to 73 microns, hall flow rate of 19 seconds and density of 7.34 grams per cm³. These results suggest that it should not have much issue with spreading as it is similar to other powder used in literature such as Inconel and Stainless Steel.

One study has shown that the typical range for Inconel powder used in laser powder bed fusion is between 15µm to 63µm [12], and that is close to the measured size range of the Neodymium powder. Inconel's hall flow rate of 28 seconds also suggest that the measured Neodymium powder will likely flow well too, since it has a quicker flow rate.

Characterisation Technique	Parameter	CoC	Bottle 01	Bottle 02	Average
Malvern Morphologi G3	Sample Mean (µm), D[4,3]	-	-	-	-
	Span	-	-	-	-
	H5 Circularity Mean, D[4,3]	-	-	-	-
Laser Diffraction Method CoC uses Microtrac Laser Analyser ARTC: Horiba LA-960 LPS	Sample Mean (µm)	-	42.95	44.72	43.835
	Span	-	1.3	1.28	1.29
	D10 (µm)	-	17.74	20.52	19.13
	D50 (µm)	Range: 35-55	40.41	44.25	42.33
	D90 (µm)	-	69.84	77.15	73.495
-	Distribution Width (1 Sigma) (t%) Formula: (D84%-D16%)/2	Range: 10-30	19.77	21.155	20.4625
	Hall Flow	Relative Hall Flow Rate (s/50g)	19.66	18.8	19.23
Hausner's Ratio	Tapped Density/Apparent Density	-	1.15	1.14	1.145
Revolution Powder Analyser	Avalanche Angle	-	42.1	41.23	41.665
	Basic Flowability Energy (mj)	-	481	438	459.5
FT4 Powder Rheometer	Stability Index	-	1.049	0.96	1.0045
	Flow Rate Index	-	1.18	1.12	1.15
	Specific Energy (mj/g)	-	1.92	1.64	1.78
	Parts per million (ppm)	-	41.23	45.24	43.235
Hall Flow	Apparent density	Range: 3.6-4.2	4.14	4.17	4.155
	Tap Density	-	4.76	4.76	4.76
-	Hausner Ratio	-	1.15	1.14	1.15
	Multi-Pycnometer	True Density (g/cm ³)	7.43 (theoretical)	7.34	7.34

Fig. 7 Summary of results for MQP-S in virgin condition

The same set of tests have been completed for MQP-S collected for reuse. It was found that there was an increase in particle size observed after just one time of recycling. Majority of virgin and recycled powders still showed good sphericity, with some elongated particles and satellite particles found.

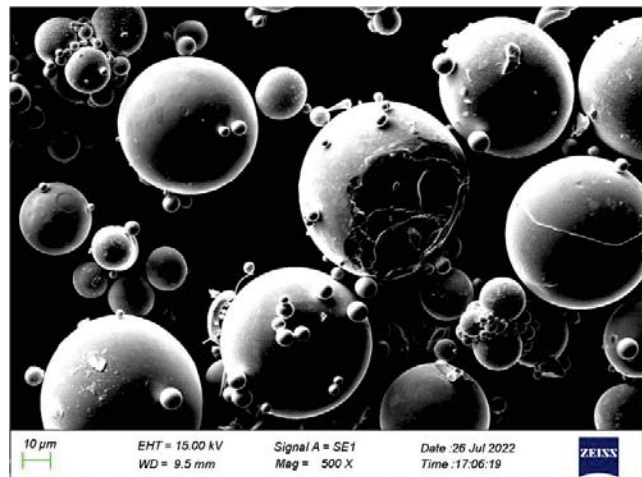


Fig. 8 SEM image of recycled powder with satellite particles

3. Conclusion

The utilization of the powder characterisation results will be useful in later parts of the research where we can use above data to conduct data-driven modification of the powder if needed, identify trends, understand final part properties and limitations of topology optimisation of part design.

An example of the use of powder characterisation data would be to correlate powder characteristics such as the sphericity of the powder against the spreading performance of powder in the LPBF machine. For example, a measured increase of elongated particles as shown in the figure below using microscopy methods (i.e., Malvern Morphologi G3) can explain streaks which sometimes are observed when attempting to print using LPBF methods.

Understanding the underlying reason for observed phenomenon is important to guide follow-up actions in attempt to remedy the

challenge faced. For example, the size range where many elongated particles are identified using microscopy can be removed by sieving as the identified sieve size based on the measurement results. Another example would be if the measured high moisture content was observed to correlate against poor flowability, the user could use this data to drive efforts to dry the powder and reassess for drying efficiency and observed improvement in flowability after drying. Other measures of powder characteristics such as flowability and moisture can also be used as indicators of flow behaviour during spreading and potentially explain any observed phenomena with the spreading of powder during the LPBF process.

Powder characterisation work can even be extended to aid in simulation studies such as in Discrete Element Method (DEM) simulation. In a few separate studies I was involved in, this area was investigated, and DEM has been shown to be able to model both Hall flow and Revolution Powder Analyser (RPA) to predict some powder intrinsic properties, like flowability, friction. In RPA, factors for the powder dynamics behaviour were mainly intrinsic properties, such as size, material property, frictional mechanics, etc [13, 14]. Therefore, it is a suitable tool to test and predict powder properties. Future work could be the incorporating of more complicated factors such as powder shape and adhesion interaction in DEM to achieve a more realistic representation.

ACKNOWLEDGEMENT

We gratefully thank the Advanced Remanufacturing and Technology Centre (ARTC) and National University Singapore (NUS) for the generous support offered.

REFERENCES

1. R. Skomski, "Permanent Magnets: History, Current Research, and Outlook," Springer International Publishing, 2016, pp. 359-395.
2. J. Cui *et al.*, "Current progress and future challenges in rare-earth-free permanent magnets," *Acta Materialia*, vol. 158, pp. 118-137, 2018.
3. J. Jacimovic *et al.*, "Net Shape 3D Printed NdFeB Permanent Magnet," (in English), *Adv. Eng. Mater.*, Article vol. 19, no. 8, p. 7, Aug 2017, Art no. 1700098, doi: 10.1002/adem.201700098.
4. J. J. Deng, Y. Q. Zhang, S. Wang, Z. P. Wang, and Y. Yang, "The Design and Coupler Optimization of a Single-Transmitter Coupled Multireceiver Inductive Power Transfer System for Maglev Trains," (in English), *IEEE Trans. Transp. Electr.*, Article vol. 7, no. 4, pp. 3173-3184, Dec 2021, doi: 10.1109/tte.2021.3061156.
5. C. Vakifahmetoglu, B. Hasdemir, and L. Biasetto, "Spreadability of Metal Powders for Laser-Powder Bed Fusion via Simple Image Processing Steps," *Materials*, vol. 15, no. 1, p. 205, 2021.
6. Magnequen. "MQP-S-11-9-20001 Powder Datasheet." <https://mqjtechnology.com/product/mqp-s-11-9-20001/>
7. F. Bittner, J. Thielsch, and W.-G. Drossel, "Laser powder bed fusion of Nd-Fe-B permanent magnets," *Progress in Additive Manufacturing*, vol. 5, no. 1, pp. 3-9, 2020.
8. N. Emminghaus, C. Hoff, J. Hermsdorf, and S. Kaierle, "Laser Powder Bed Fusion of NdFeB and influence of heat treatment on microstructure and crack development," *Procedia CIRP*, vol. 94, pp. 211-216, 2020.
9. J. L. Wu, N. T. Aboulkhair, M. Degano, I. Ashcroft, and R. J. M. Hague, "Process-structure-property relationships in laser powder bed fusion of permanent magnetic Nd-Fe-B," (in English), *Mater. Des.*, Article vol. 209, p. 11, Nov 2021, Art no. 109992, doi: 10.1016/j.matdes.2021.109992.
10. C. Huber, G. Mitteramskogler, M. Goertler, I. Teliban, M. Groenefeld, and D. Suess, "Additive Manufactured Polymer-Bonded Isotropic NdFeB Magnets by Stereolithography and Their Comparison to Fused Filament Fabricated and Selective Laser Sintered Magnets," (in English), *Materials*, Article vol. 13, no. 8, p. 8, Apr 2020, Art no. 1916, doi: 10.3390/ma13081916.
11. M. Balbaa, A. Ghasemi, E. Fereiduni, M. Elbestawi, S. Jadhav, and J.-P. Kruth, "Role of powder particle size on laser powder bed fusion processability of AlSi10Mg alloy," *Additive Manufacturing*, vol. 37, p. 101630, 2021.
12. Q. B. Nguyen, M. L. S. Nai, Z. Zhu, C.-N. Sun, J. Wei, and W. Zhou, "Characteristics of inconel powders for powder-bed additive manufacturing," *Engineering*, vol. 3, no. 5, pp. 695-700, 2017.
13. L. Dai, Y. Chan, G. Vastola, N. Khan, S. Raghavan, and Y. Zhang, "Characterizing the intrinsic properties of powder—a combined discrete element analysis and Hall flowmeter testing study," *Advanced Powder Technology*, vol. 32, no. 1, pp. 80-87, 2021.
14. L. Dai, Y. Chan, G. Vastola, and Y. Zhang, "Discrete element simulation of powder flow in revolution powder analyser: Effects of shape factor, friction and adhesion," *Powder Technol.*, p. 117790, 2022.